Supporting Information

Direct Hydrogen Selenide (H₂Se) Release from Activatable Selenocarbamates

Turner D. Newton,[1,#] Keyan Li,[1,#] Jyoti Sharma,[2] Pier Alexandre Champagne,[2] and Michael D. Pluth[1,*]

[1] Department of Chemistry and Biochemistry, Materials Science Institute, Knight Campus for Accelerating Scientific Impact, and Institute of Molecular Biology, University of Oregon, Eugene, Oregon, 97403-1253, USA.

[2] Department of Chemistry and Environmental Science, New Jersey Institute of Technology, Newark, New Jersey, 07103, USA.

# These authors contributed equally to this work.

*Corresponding author

e-mail: pluth@uoregon.edu

Table of Contents

NMR Spectra

Figure S1. ^{1}H NMR (600 MHz, CDCl$_3$) spectrum of 4-nitrophenyl isoselenocyanate.

Figure S2. ^{13}C{^{1}H} NMR (151 MHz, CDCl$_3$) spectrum of 4-nitrophenyl isoselenocyanate.
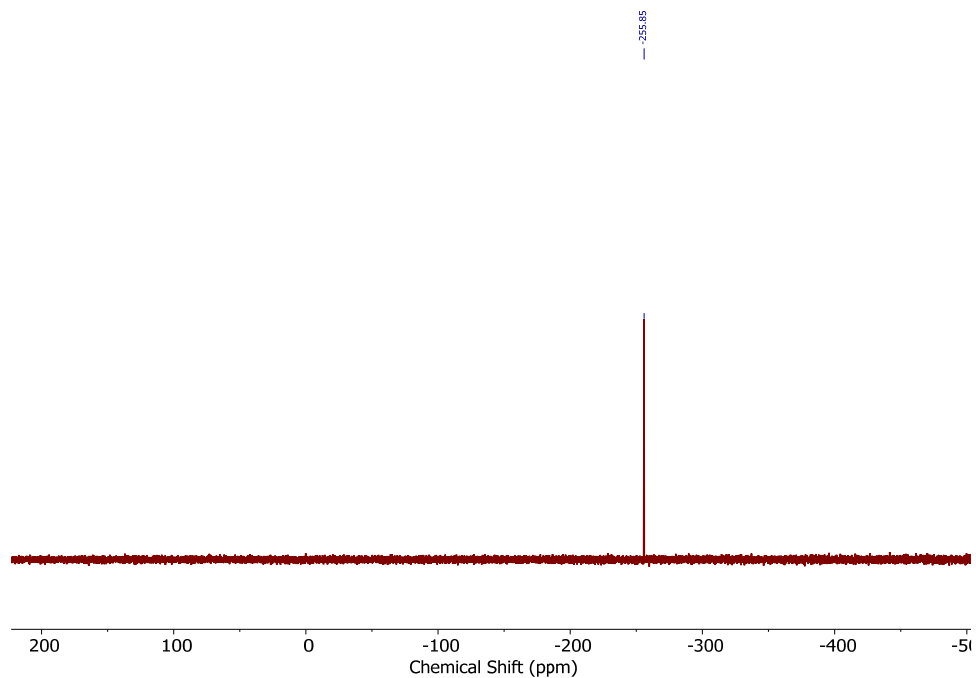
Figure S3. ^{77}Se NMR (115 MHz, CDCl$_3$) spectrum of 4-nitrophenyl isoselenocyanate.
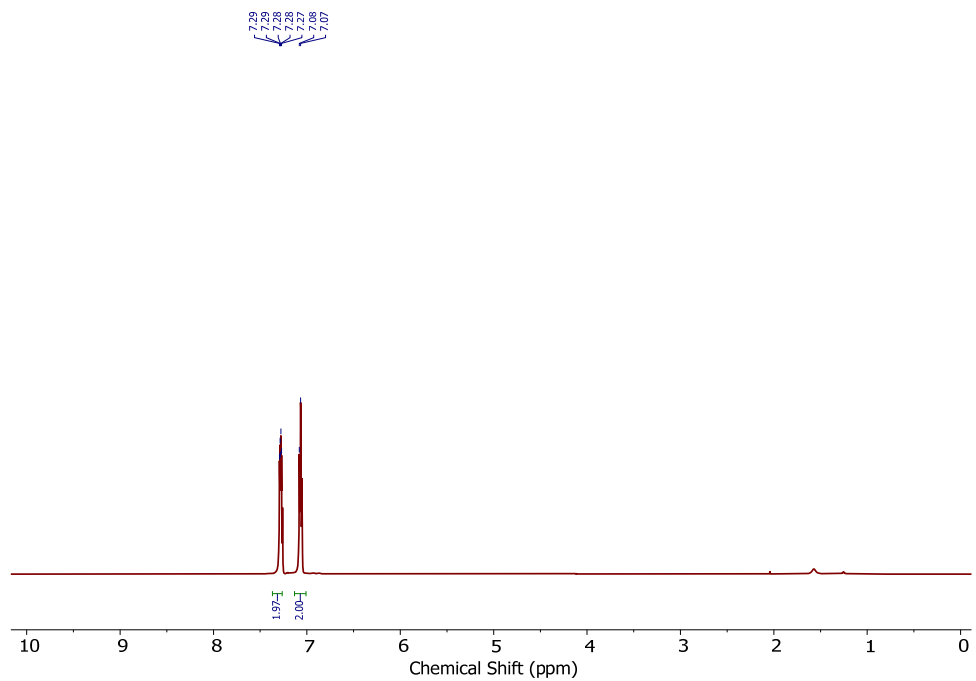
Figure S4. ^{1}H NMR (600 MHz, CDCl$_3$) spectrum of 4-fluorophenyl isoselenocyanate.
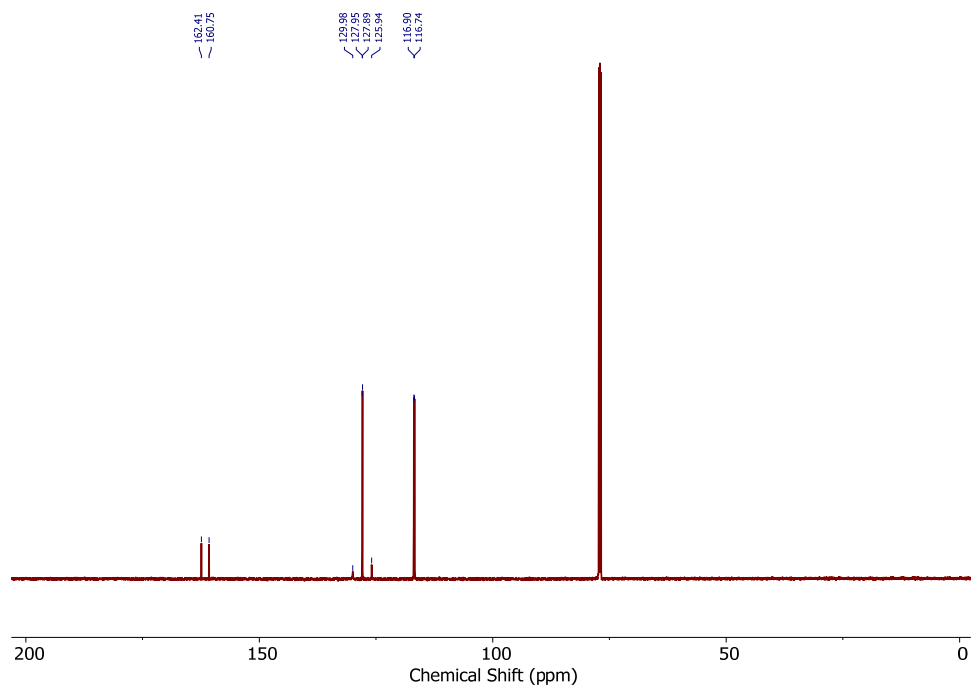
Figure S5. $^{13}C\{^{1}H\}$ NMR (151 MHz, CDCl$_3$) spectrum of 4-fluorophenyl isoselenocyanate.
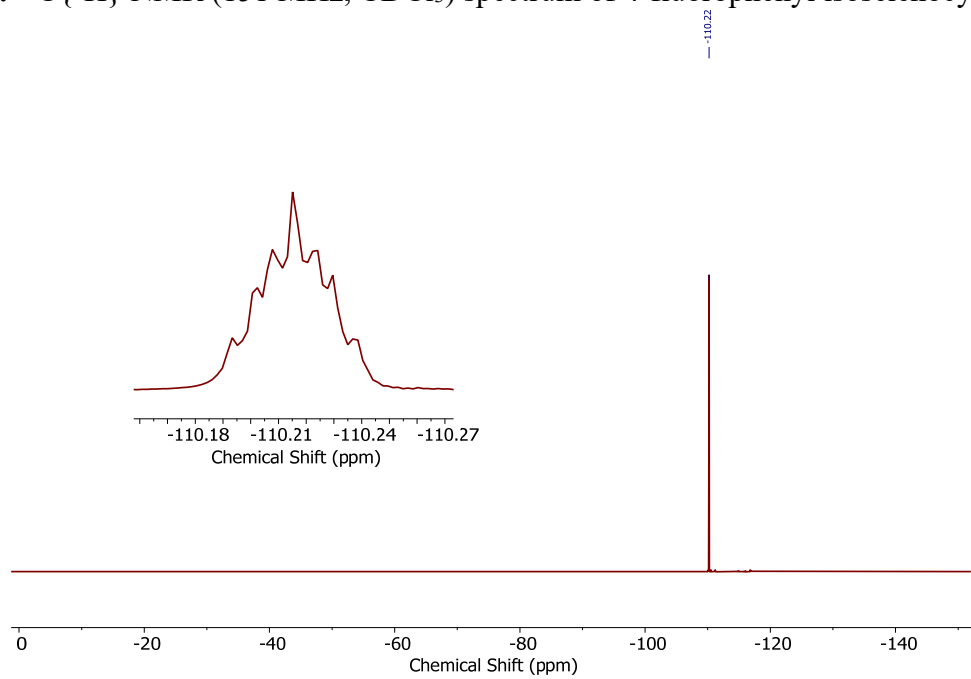
Figure S6. ^{19}F NMR (564 MHz, CDCl$_3$) spectrum of 4-fluorophenyl isoselenocyanate.
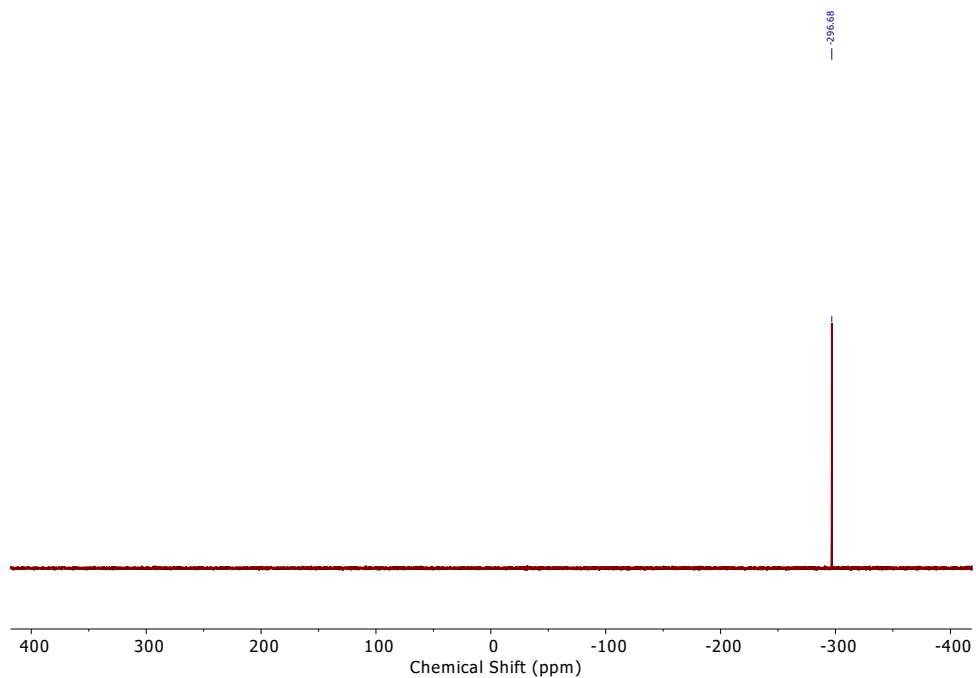
Figure S7. ^{77}Se NMR (115 MHz, CDCl$_3$) spectrum of 4-fluorophenyl isoselenocyanate.
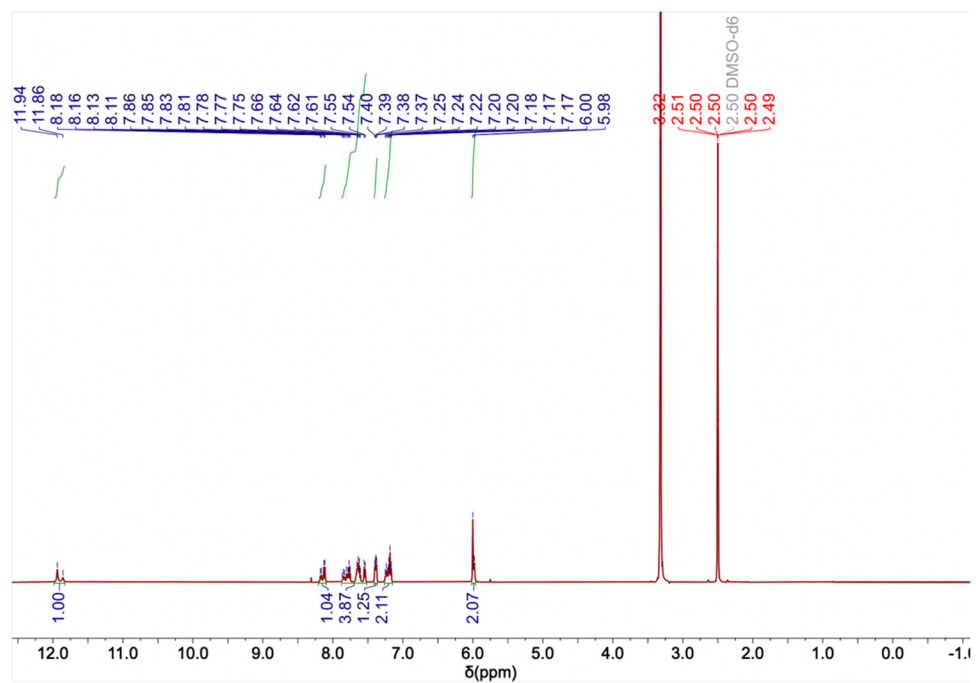
Figure S8. ^{1}H NMR (600 MHz, DMSO-d$_6$) spectrum of PhotoSeCM.
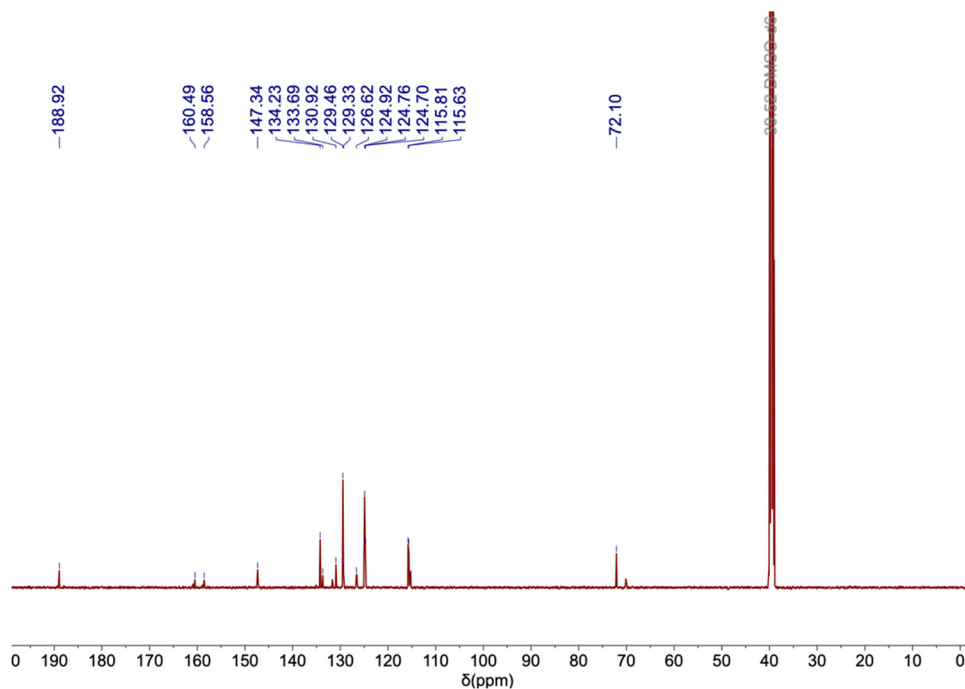
Figure S9. $^{13}C\{^1H\}$ NMR (151 MHz, DMSO-d$_6$) spectrum of PhotoSeCM.
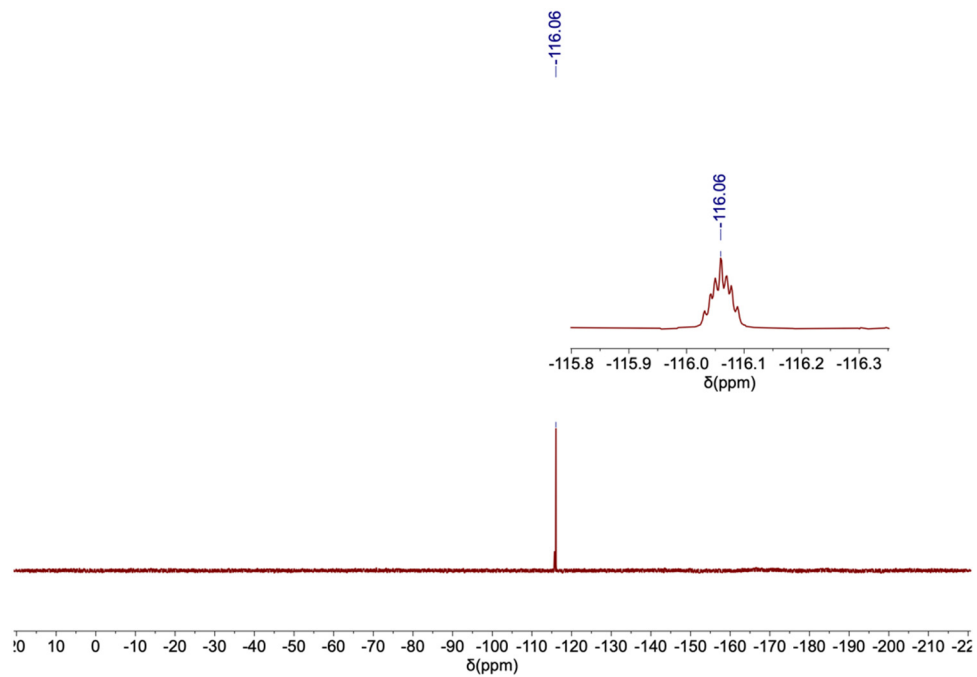
Figure S10. ^{19}F NMR (564 MHz, DMSO-d$_6$) spectrum of PhotoSeCM.
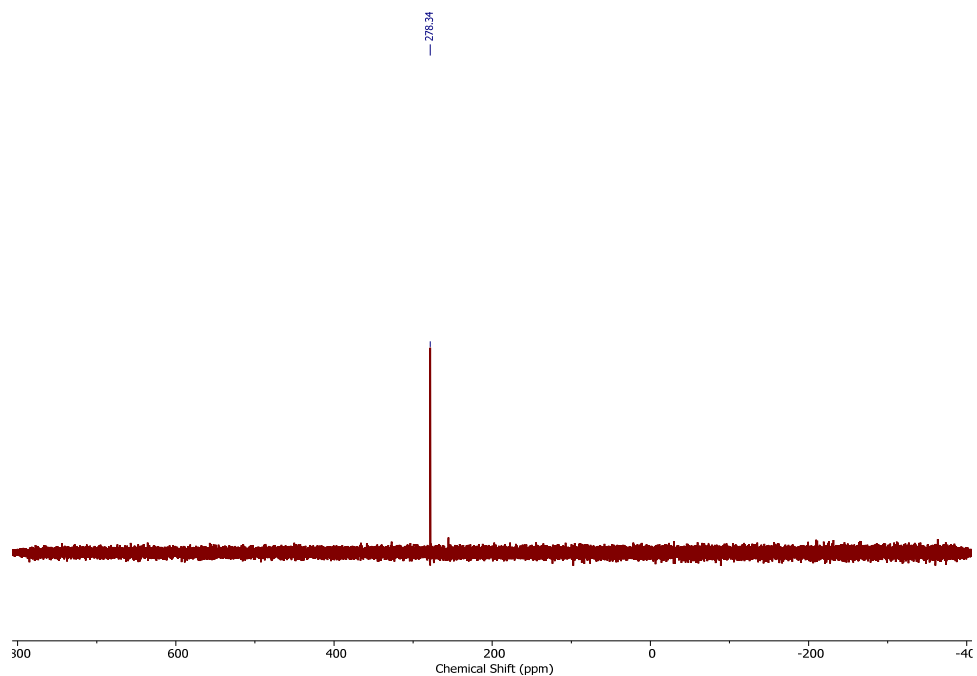
Figure S11. ^{77}Se NMR (115 MHz, DMSO-d$_6$) spectrum of PhotoSeCM.
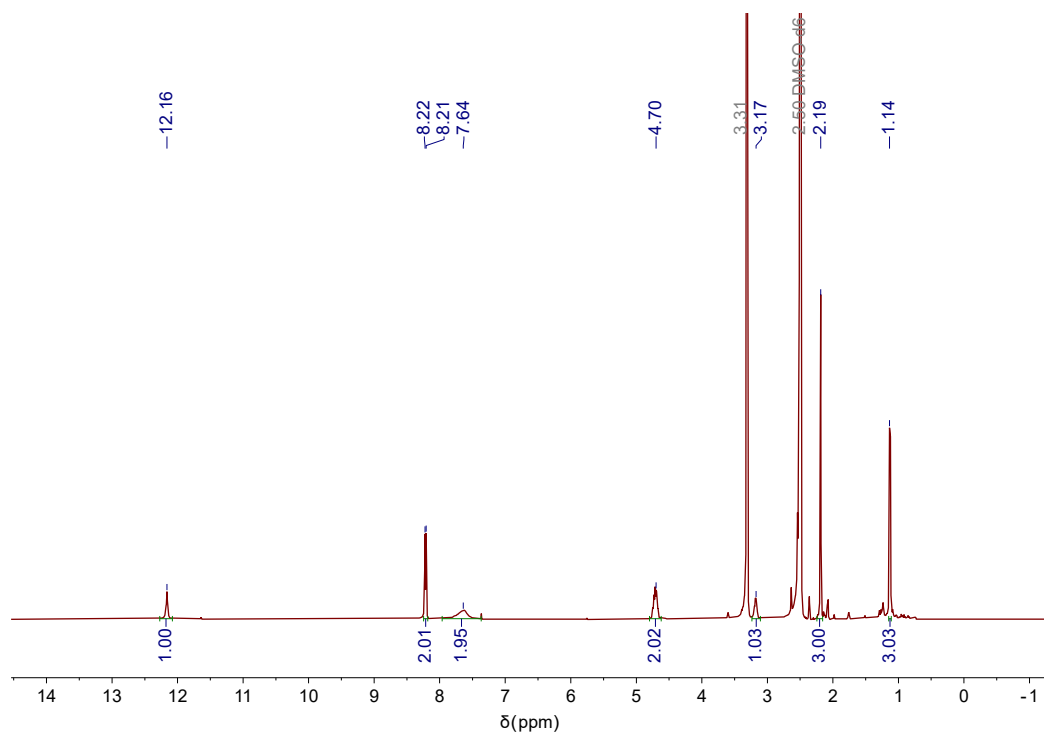
Figure S12. ^{1}H NMR (600 MHz, DMSO-d$_6$) spectrum of PNA-MeGKSeCM.
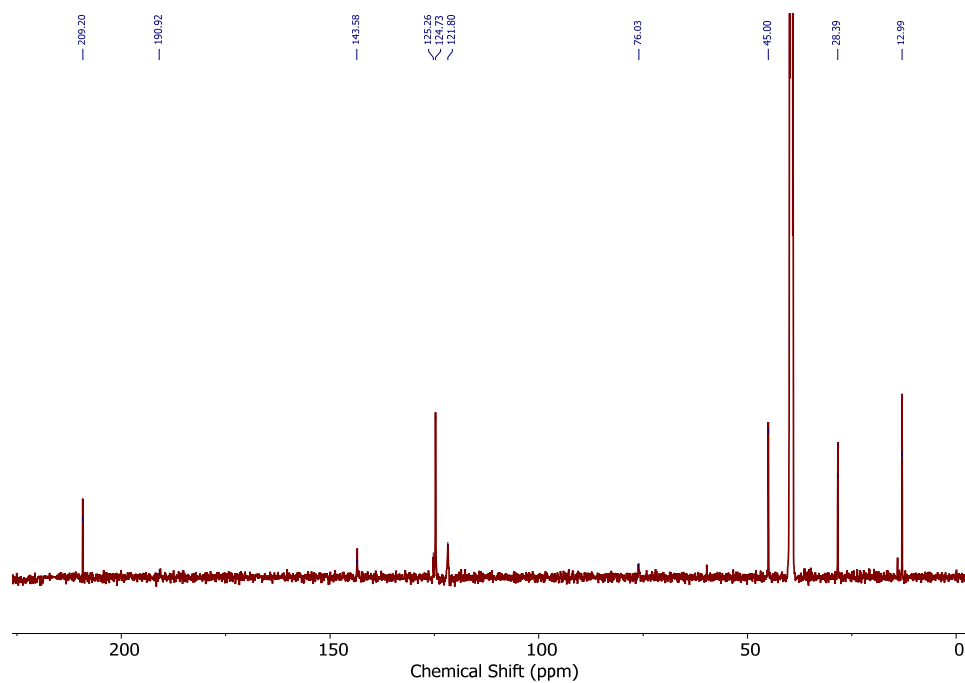
Figure S13. $^{13}C\{^1H\}$ NMR (151 MHz, DMSO-d$_6$) spectrum of PNA-MeGKSeCM.
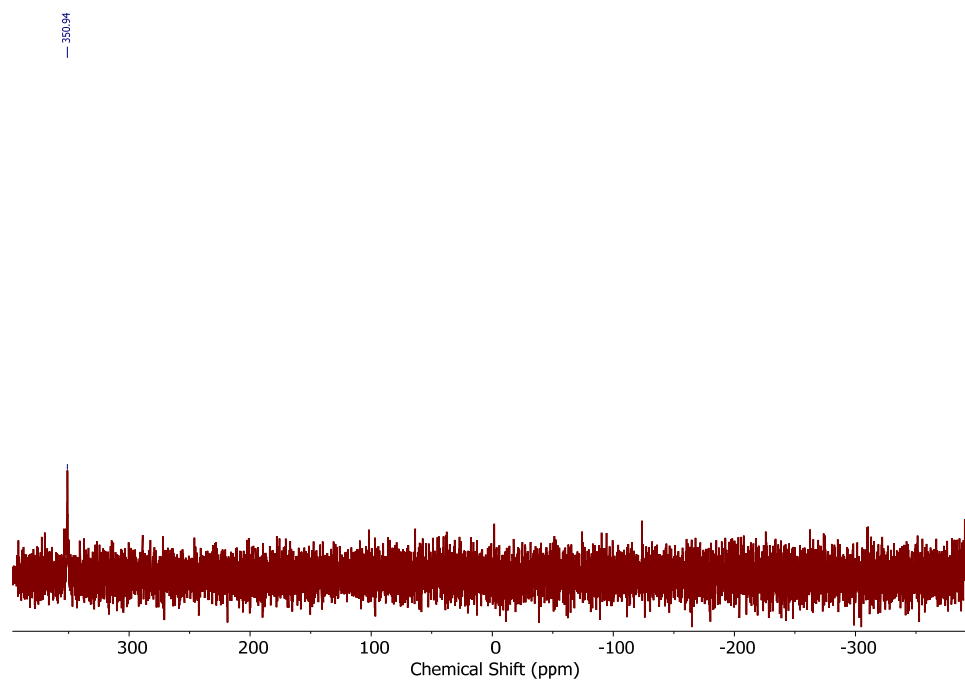
Figure S14. ^{77}Se NMR (115 MHz, DMSO-d$_6$) spectrum of PNA-MeGKSeCM.
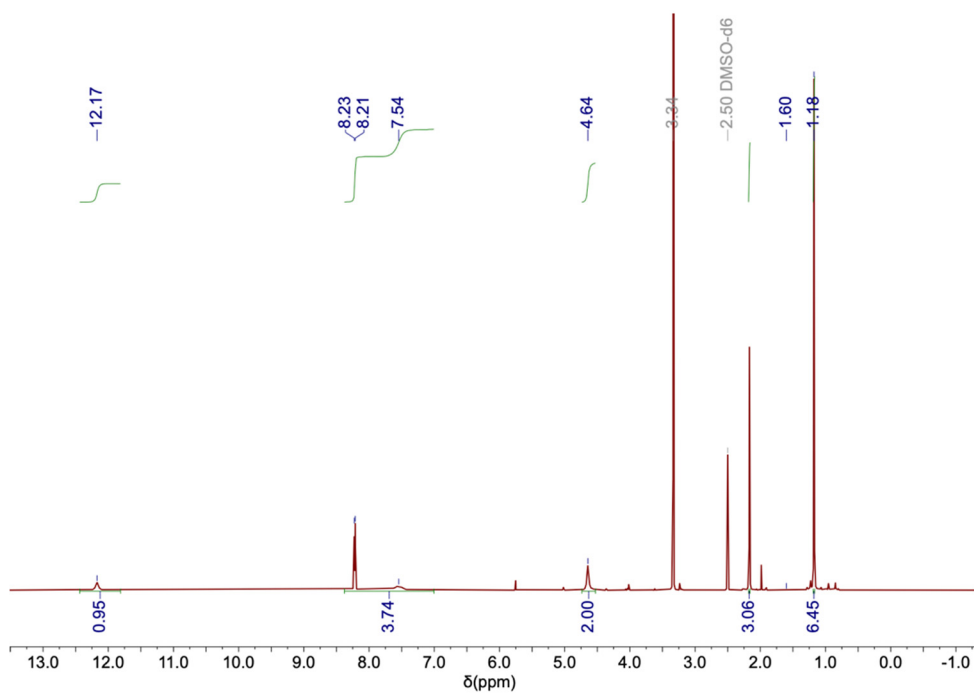
Figure S15. ^{1}H NMR (600 MHz, DMSO-d$_6$) spectrum of PNA-Me$_2$GKSeCM.
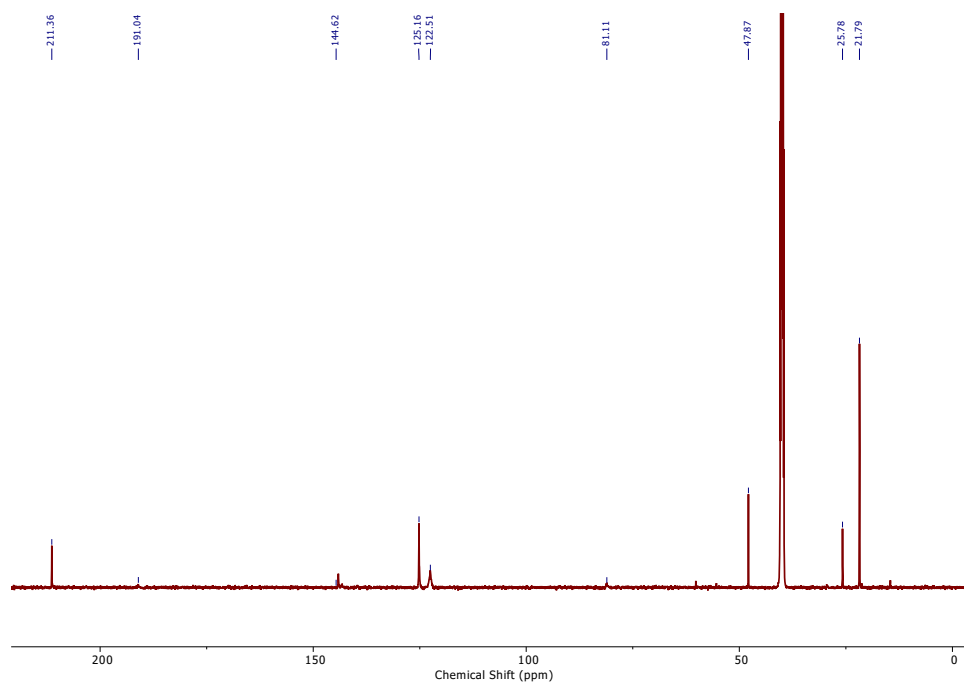
Figure S16. ^{13}C{^{1}H} NMR (151 MHz, DMSO-d$_6$) spectrum of PNA-Me$_2$GKSeCM.

─352.81
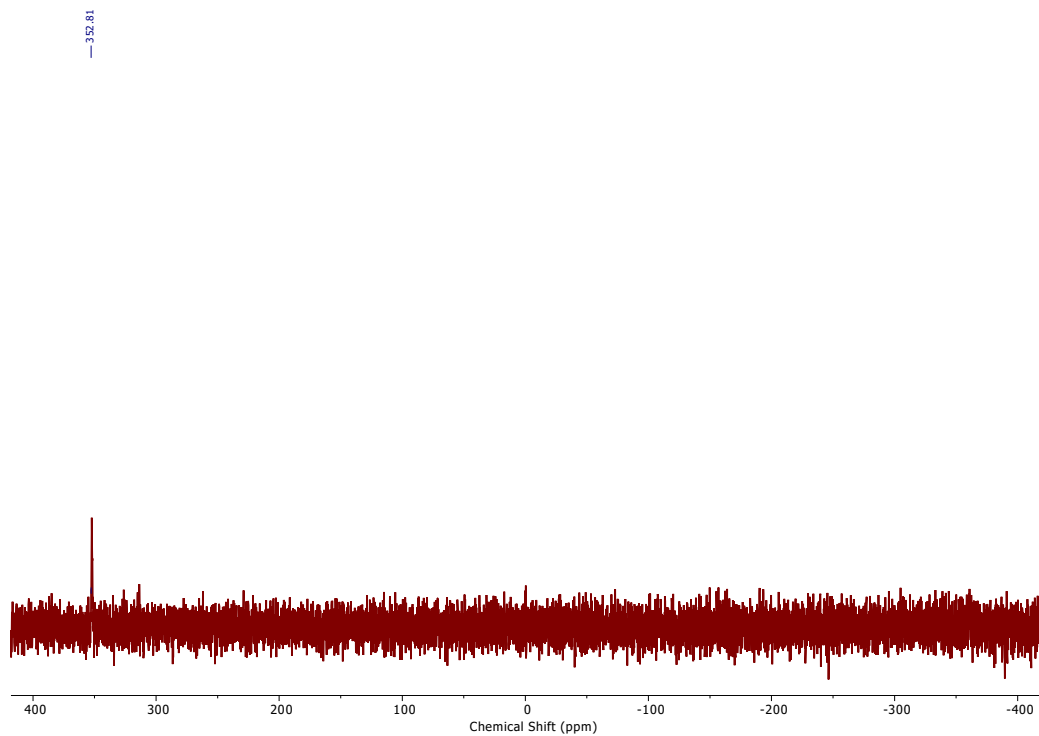
Figure S17. ^{77}Se NMR (115 MHz, DMSO-d$_6$) spectrum of PNA-Me$_2$GKSeCM.

─40.30
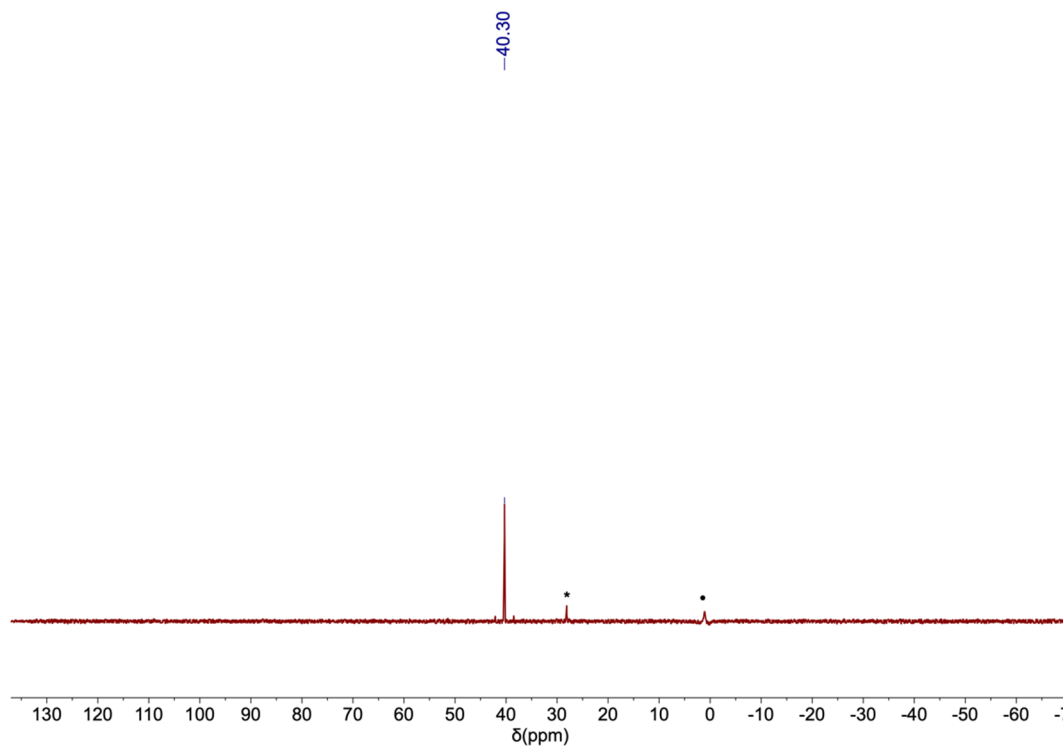
Figure S18. ^{31}P NMR (242 MHz, MeCN-d$_3$) spectrum of H$_2$Se trapping mixture after treatment with PPh$_3$, showing Se=PPh$_3$ formation. "*" denotes trace O=PPh$_3$ byproduct and "•" denotes residual PPh$_3$.
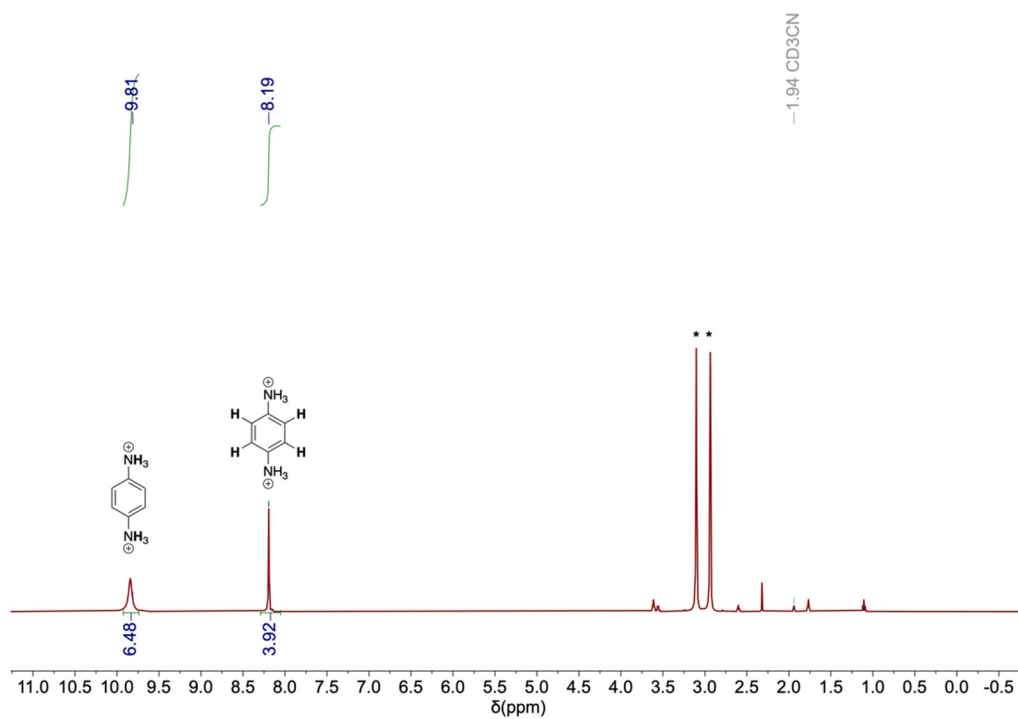
Figure S19. ^{1}H NMR (500 MHz, MeCN-d$_3$) spectrum of H$_2$Se trapping mixture. "*" denotes DMF.
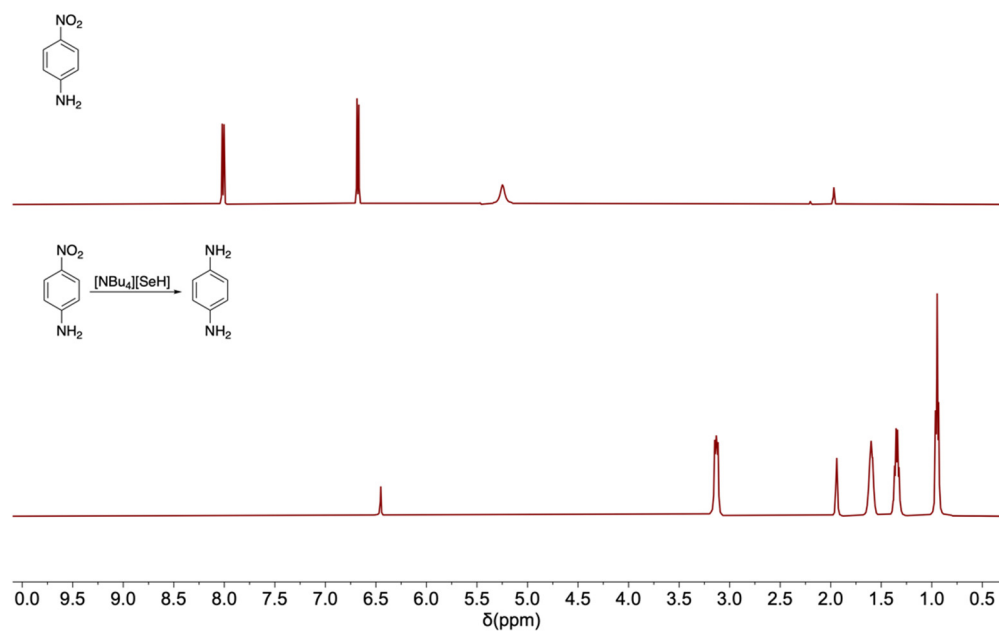
Figure S20. ^{1}H NMR (500 MHz, MeCN-d$_3$) spectra of *p*-nitroaniline standard (top) and *p*-nitroaniline treated with [NBu$_4$][SeH] to produce *p*-phenylenediamine (bottom).
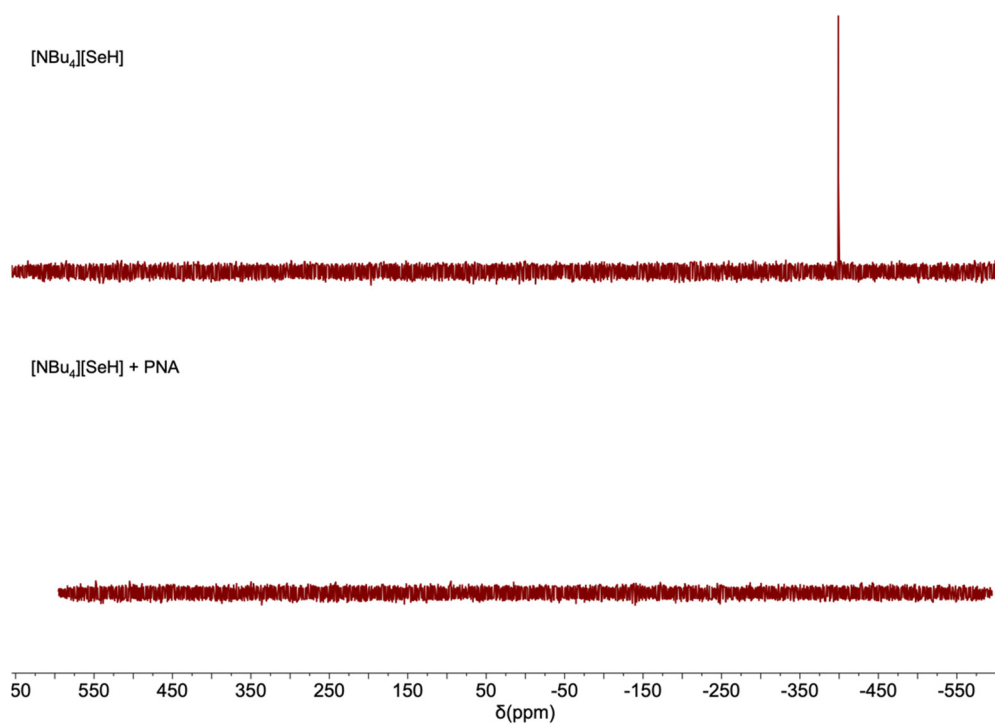
Figure S21. ^{77}Se NMR (115 MHz, MeCN-d$_3$) spectra of [NBu$_4$][SeH] (top) and [NBu$_4$][SeH] treated with *p*-nitroaniline (bottom).

Full computational details

Gaussian 16 was used to perform Density Functional Theory (DFT) calculations,[1] where geometry optimizations were conducted with the ωB97X-D[2] method using the aug-cc-pVDZ basis set.[3] Following this, single-point energy refinements were performed using the ωB97X-D functional and the aug-cc-pV(T+d)Z basis set. The SMD implicit solvation model for water was used at all stages to consider solvation effects.[4] By default, Gaussian 16 request an "ultrafine" pruned (99,590) grid for numerical integrations, eliminating most orientation-specific issues.[5] Frequency calculations were performed at the optimization level to confirm stationary points as minima or first-order saddle points and obtain corrections for zero-point energy, enthalpy, and free energy at a standard state of 1 atm pressure and 298 K temperature using Goodvibes v2.0.3.[6] Grimme's scheme for the treatment of small frequencies was applied, setting frequencies below 100 cm^{-1} to 100 cm^{-1}.[7] The final free energies were computed by adding the free energy corrections obtained from the frequency analysis to the single-point electronic energies. CYLview was used to prepare visualizations of the computed structures.[8]

Estimation of free energies of protonation of anionic species

The free energy of protonation of the anionic species was evaluated using two methods. In the first method, the free energy of reaction for using water and forming hydroxide was evaluated using the energies of the isolated species. For species that have a known pK_a in water, the free energy of deprotonation was computed from the pH of the solution using the following relationship:[9]

$$\Delta G_{deprot} = -RT \ln\left(10^{(pH-pK_a)}\right) = RT\ (pK_a - pH) \ln(10)$$

For phenylcarbamic acid (PhNCO$_2$H), which has a known pK_a of 4.62, we compute that the free energy of protonation of **4b** at pH 8 and 298.15 K is 4.6 kcal/mol, which is the value shown in Figure 8 for the transformation of **4b** to **5a**. For the same transformation, using an isolated water and forming an isolated hydroxide in DFT calculations, a value of 26.4 kcal/mol is obtained. This large difference can be caused by the fact that this hypothetical reaction does not consider explicit solvation of water and hydroxide, and that it represents the maximum basicity of one hydroxide molecule without hydrogen bonding.

For *p*-nitrophenylcarbamic acid that has a pK_a of 1.2, at pH 8 the protonation of the carbamate has a reaction free energy of 9.3 kcal/mol.

The difference between the pK_a- and DFT-computed values for protonation of **4b** (21.7 kcal/mol) allow us to crudely estimate the pK_a of species for which no data in water exists. For instance, for anilide protonation with an isolated water has a reaction energy of -5.1 kcal/mol (shown in Figure 8). By comparison with the phenylcarbamic acid, this free energy difference at pH 8 should be -26.8, giving a pK_a of anilide at 27.7, in line with its pK_a in DMSO (30.6). Due to the obvious limitations of this method considering the approximations, we prefer to use the DFT-computed value in Figure 8.

Transition state structures of COSe, HSe⁻, and H₂O release from selenocarbamate tautomers

The potential energy diagrams for path 1 and path 2 are presented in the main text. Path 2, in the presence of an explicit water molecule (TS1'), is higher in free energy than TS1 by 0.8 kcal/mol and as such presents no free energy benefit.

Path 1

Path 2

(possible assisted
pathways including
H₂O or H₂PO₄⁻)
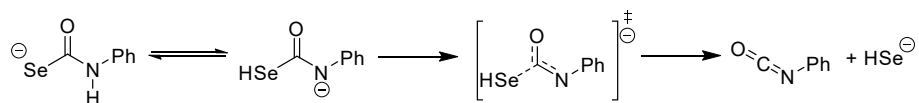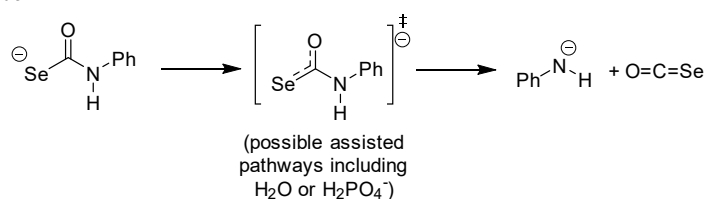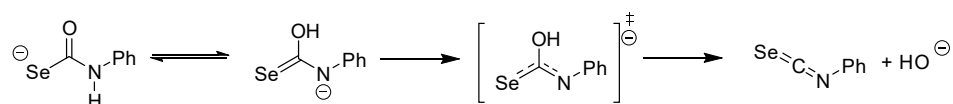
Path 3

Scheme S1. Competing pathways for H₂Se, COSe and H₂O release.

TS1   TS1'   TS2
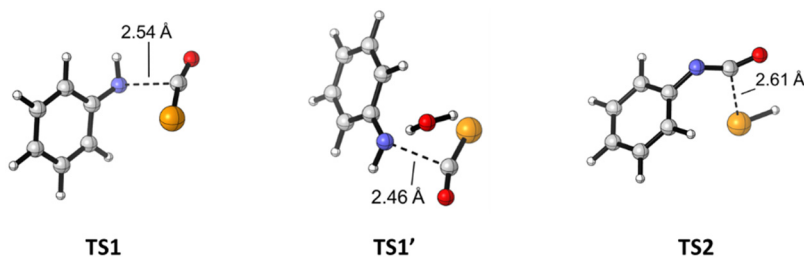
Figure S22. TSs for selenocarbamate **3** associated with paths 1 and 2.

3a [0.0]   3c [14.4]   TS 3c [53.0]   [35.8]   TS 3c
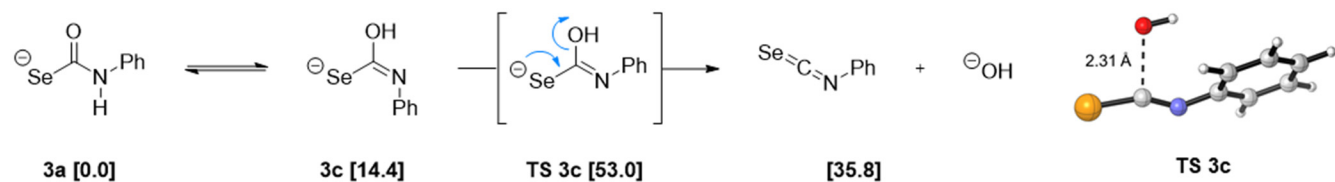
Figure S13. Potential energy surface (PES) for path 3

Protonation of 3a for the release of COSe

The protonation of **3a** to form **3a·H** was studied using an isolated water molecule (**Figure S24**). For the most stable protonation to **3a·H (SeH)**, the reaction energy is 29.4 kcal/mol, which amounts to 7.7 kcal/mol at pH 8 if estimated based on the difference found for phenylcarbamic acid (see above). This energy difference gives an estimated pK_a of 2.4 for **3a**, less basic than dithiocarbamates.[10] For a *p*-nitroselenocarbamate, this pK_a would go down to -1.0, by comparison to the carbamate. The zwitterionic **3a·H (NH₂)** is 11.9 kcal/mol higher in free energy than **3a·H (SeH)**, and so sits at 19.6 kcal/mol (assuming the pH 8 correction). The TS for elimination of COSe and aniline is then 2.4 kcal/mol higher in free energy.
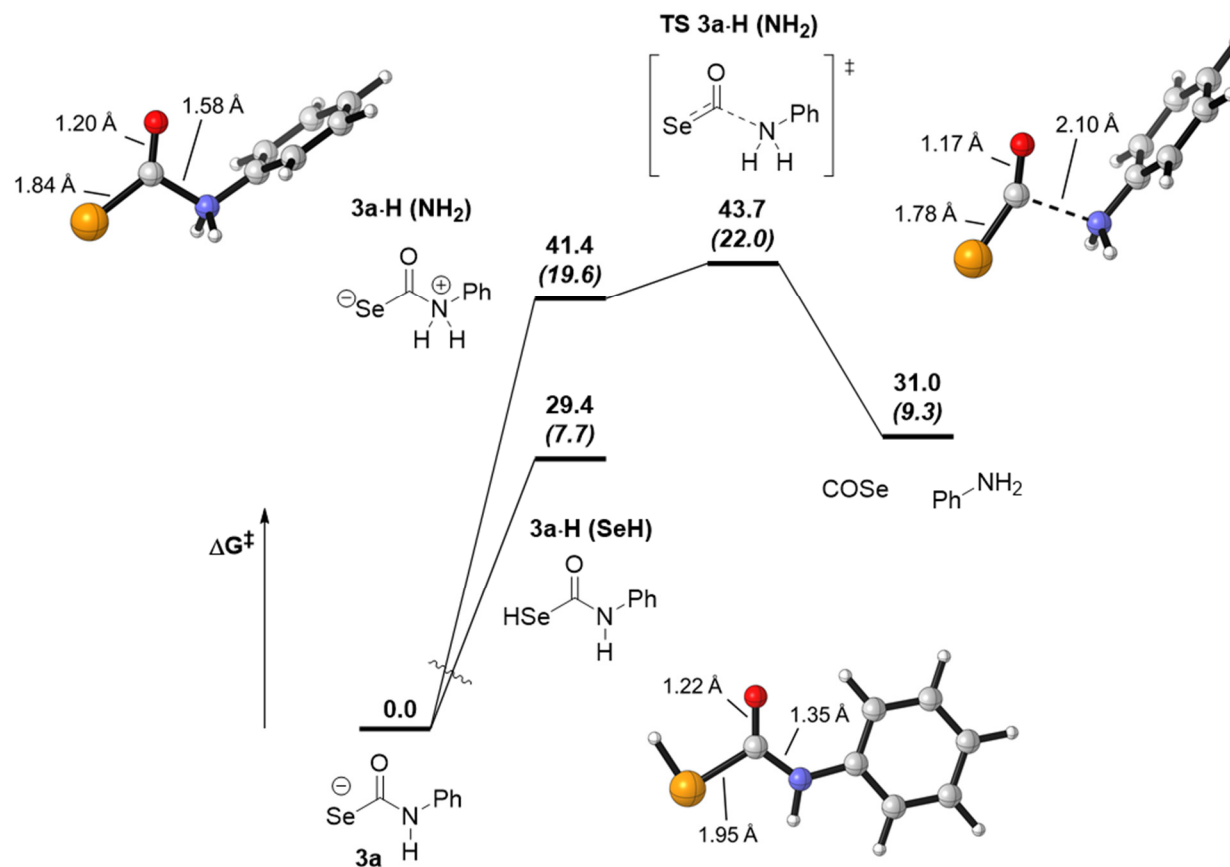
Figure S24. Protonation of **3a** and subsequent elimination of COSe and aniline. Free energies (in kcal/mol) represent the protonation from water forming hydroxide (top value), and the estimated value at pH 8 considering the free energy difference found for phenylcarbamic acid (italics, see above).

Release of Aniline and carbon dioxide from phenyl isocyanate.

We have designed several reaction pathways to investigate the ultimate product synthesis of aniline and carbon dioxide, as presented in Scheme S1. The associated activation and reaction energies are depicted in Table S7. According to our computational analysis, the lowest energy barrier associated with the hydroxy anion (OH⁻) attacking phenylisocyanate is 11.0 (TS3) The resulting product **4a** generates a CO_2 by tautomerization to **4b**, ultimately leading to cleavage and formation of the anilide anion and CO_2 via two potential transition states, namely **TS4** and **TS4'** (in the presence of explicit water). Our calculations show that **TS4** exhibits a lower activation barrier compared to **TS4'** because of the presence of a water molecule that causes entropy loss. A more reasonable pathway for the generation of aniline and CO_2 is from **5b** via **TS5**. As shown in the main text, this pathway has a lower free energy requirement, especially if the protonation free energy for **4b** is computed for pH 8 using the experimental pK_a.
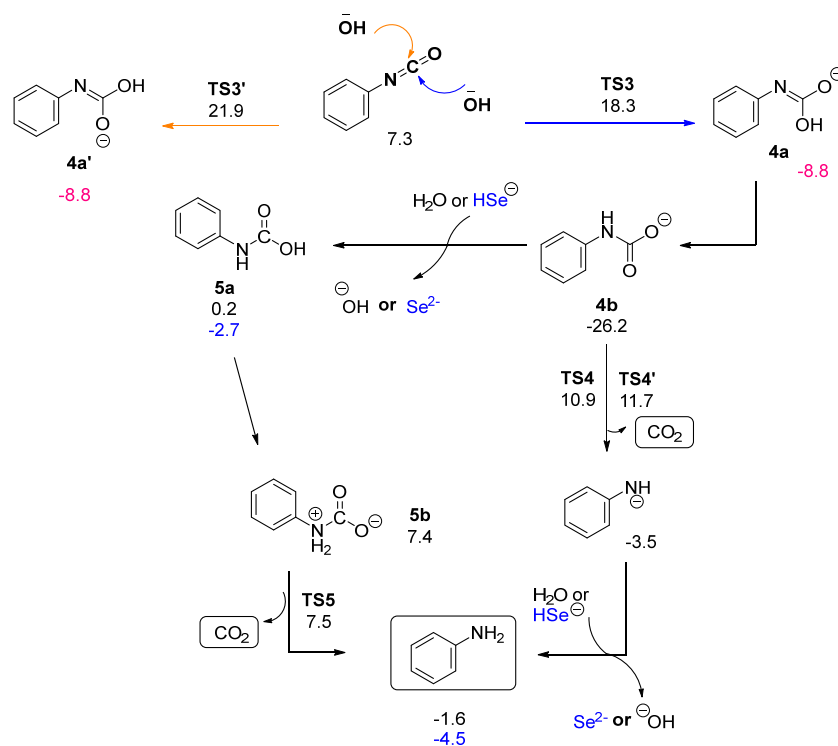
Scheme S2. Possible routes for elimination of aniline and carbon dioxide. All free energies are presented relative to **3a** (0.0 kcal/mol).
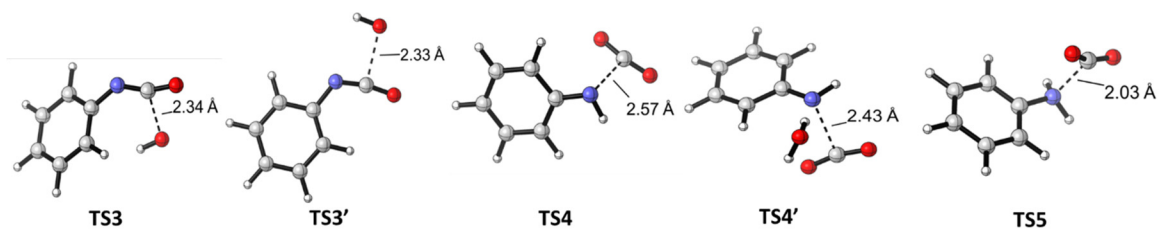
Figure S25. TSs for formation of aniline and carbon dioxide from phenylisocyanate.

Energy, thermochemical correction, and ωB97X-D single-point refinements of all structures.

All thermochemical corrections were obtained using the optimization level of theory (ωB97X-D/aug-cc-pVDZ/SMD(H₂O)) at the standard state of 1 atm and 298.15 K, using Grimme's quasiharmonic corrections. Single-point energy refinements were obtained at the ωB97X-D/aug-cc-pV(T+d)Z/SMD(H2O) level of theory.

Table S1. Energies (E), enthalpies (H), quasi-harmonic-corrected free energies (G), and single-point energies (SPE) of ground state structures (in hartrees).

Structure	E	H	G	ωB97X-D SPE
CO_2	-188.546602	-188.531463	-188.555723	-188.593854
COSe	-2514.89787	-2514.885722	-2514.91346	-2514.998045
H_2O	-76.431113	-76.405966	-76.427396	-76.451362
HSe anion	-2402.336637	-2402.327787	-2402.3504	-2402.408145
4a	-475.62769	-475.499254	-475.541304	-475.733479
4b	-475.652788	-475.52362	-475.565807	-475.759062
PhNCO	-399.640514	-399.528349	-399.568091	-399.731905
PhNCSe	-2725.997707	-2725.887861	-2725.930744	-2726.143671
anilide anion	-287.03412	-286.923955	-286.959143	-287.096895
hydroxide	-75.933259	-75.92112	-75.940672	-75.951852
Se dianion	-2401.851633	-2401.849272	-2401.867826	-2401.921936
Aniline	-287.550379	-287.426114	-287.461889	-287.60687
5a	-476.109994	-475.967169	-476.009425	-476.219023
5b	-476.098169	-475.955331	-475.998049	-476.207155

Table S2. Energies (E), enthalpies (H), quasi-harmonic-corrected free energies (G), and single-point energies (SPE) of ground state selenocarbamate tautomers and protonated selenocarbamic acids (in hartrees)

Structure	E	H	G	ωB97X-D SPE
3a	-2802.01661	-2801.88896	-2801.933372	-2802.176284
3b	-2801.9824	-2801.860318	-2801.90598	-2802.141503
3c	-2801.993725	-2801.866674	-2801.911302	-2802.152839
3a·H (NH₂)	-2802.449046	-2802.308503	-2802.353868	-2802.610748
3a·H (SeH)	-2802.462951	-2802.326296	-2802.37214	-2802.625342

Table S3. Energies (E), enthalpies (H), quasi-harmonic-corrected free energies (G), and single-point energies (SPE) of transition states from selenocarbamate tautomers and protonated forms (in hartrees).

Structure	E	H	G	ωB97X-D SPE
TS-1	-2801.932923	-2801.810191	-2801.856201	-2802.094787
TS-2	-2801.971713	-2801.850984	-2801.896926	-2802.132687
TS 3c	-2801.923198	-2801.800754	-2801.84721	-2802.084566
TS 3a·H (NH₂)	-2802.439642	-2802.302	-2802.347971	-2802.60338

Table S4. Energies (E), enthalpies (H), quasi-harmonic-corrected free energies (G), and single-point energies (SPE) of transition state structures involve in aniline and carbon dioxide formation (in hartrees).

Structure	E	H	G	ωB97X-D SPE
TS3	-475.573896	-475.448979	-475.492655	-475.682445
TS3'	-475.567214	-475.442539	-475.487092	-475.675612
TS4	-475.58492	-475.459385	-475.503414	-475.694604
TS4'	-552.032775	-551.880527	-551.930483	-552.16165
TS5	-476.092429	-475.952107	-475.995693	-476.203636

XYZ coordinates for all the computed structures.

All structures were optimized at the ωB97X-D/aug-cc-pVDZ/SMD(H₂O) level of theory.

Imaginary frequencies are provided for all transition structures.

Ground states structures

CO₂

C	0.000000	0.000000	0.000000
O	0.000000	0.000000	1.162953
O	0.000000	0.000000	-1.162953

COSe

C	0.000000	0.000000	-1.020765
O	0.000000	0.000000	-2.178358
Se	0.000000	0.000000	0.692690

H₂O

H	-0.000000	-0.759193	-0.474324
O	0.000000	0.000000	0.118581
H	0.000000	0.759193	-0.474324

HSe anion

Se	0.000000	0.000000	0.042123
H	0.000000	0.000000	-1.432196

PhNCO

C	1.637275	1.386013	0.000048
C	0.284600	1.054395	0.000173
C	-0.091432	-0.292569	0.000153
C	0.873870	-1.300120	-0.000113
C	2.224871	-0.955132	-0.000193
C	2.611326	0.385399	-0.000162
H	1.930198	2.435855	0.000094
H	-0.478132	1.833207	0.000272
H	0.563462	-2.344154	-0.000158
H	2.978489	-1.742558	-0.000351
H	3.668172	0.650982	-0.000209
N	-1.446445	-0.674501	0.000585
C	-2.504895	-0.091863	0.000209
O	-3.593846	0.346429	-0.000554

Anilide anion

C	0.235081	-1.227917	0.000466
C	1.047535	-0.045010	0.000114
C	0.310024	1.187787	0.000474
C	-1.079759	1.222697	-0.000024
C	-1.843267	0.046622	-0.000396
C	-1.152950	-1.175206	-0.000068
H	0.738359	-2.198370	0.000943
H	0.871023	2.126890	0.001080
H	-1.583447	2.192975	0.000023
H	-2.932722	0.080138	-0.000899
H	-1.716144	-2.112109	0.000075
N	2.392750	-0.136380	-0.000541
H	2.773687	0.811298	-0.000833

Aniline

C	-1.17008	1.20292	0.00360
C	0.22327	1.20835	-0.00465
C	0.93819	-0.00010	-0.01006
C	0.22324	-1.20839	-0.00463
C	-1.17023	-1.20281	0.00367
C	-1.88034	0.00003	0.00671
H	-1.70673	2.15268	0.00963
H	0.76923	2.15324	-0.00664
H	0.76893	-2.15342	-0.00651
H	-1.70693	-2.15255	0.00971
H	-2.97014	0.00004	0.01368
N	2.33270	0.00007	-0.08094
H	2.76632	-0.83761	0.28870
H	2.76616	0.83716	0.29019

4a

C	-2.04802	-1.27113	-0.27608
C	-0.69260	-0.98718	-0.43418
C	-0.19326	0.31261	-0.22035
C	-1.11173	1.31163	0.14813
C	-2.46732	1.02437	0.30799
C	-2.94735	-0.26982	0.09916
H	-2.40660	-2.28626	-0.45414
H	-0.00766	-1.77716	-0.74306
H	-0.74808	2.32800	0.30727
H	-3.15378	1.82137	0.59803
H	-4.00721	-0.49438	0.22054
N	1.14417	0.66354	-0.44689
C	2.08568	-0.06233	0.11532
O	3.37791	0.29931	-0.24579
O	2.02907	-1.00078	0.95037
H	3.30585	1.02658	-0.87693

4b

C	2.02142	1.32009	-0.05728
C	0.65499	1.03543	-0.08808
C	0.21507	-0.29657	-0.03631
C	1.17818	-1.32030	0.04015
C	2.53615	-1.02191	0.06721
C	2.97303	0.30453	0.02094
H	2.34068	2.36233	-0.09916
H	-0.06709	1.84215	-0.15413
H	0.84772	-2.35974	0.07814
H	3.25969	-1.83577	0.12727
H	4.03686	0.53976	0.04345
N	-1.12563	-0.69021	-0.08000
C	-2.30493	0.05895	0.01766
O	-3.37385	-0.62286	-0.04927
O	-2.23869	1.30903	0.16193
H	-1.28152	-1.68795	-0.12254

5a

C	2.08190	1.31045	-0.03900
C	0.71158	1.04398	-0.06674
C	0.27031	-0.28282	-0.03077
C	1.20661	-1.32464	0.02583
C	2.56838	-1.04316	0.05022
C	3.01672	0.27901	0.02011
H	2.41577	2.34790	-0.06617
H	0.00123	1.86203	-0.11724
H	0.85982	-2.35860	0.05116
H	3.28287	-1.86519	0.09469
H	4.08339	0.50052	0.04110
N	-1.08899	-0.66554	-0.06160
C	-2.18683	0.12849	0.01616
O	-3.37436	-0.51743	-0.01358
O	-2.18829	1.34826	0.10800
H	-1.24956	-1.66534	-0.09765
H	-3.28143	-1.47717	-0.08499

5b

C	-2.20606	1.20946	-0.11530
C	-0.87284	1.21533	0.29164
C	-0.22832	-0.00001	0.48986
C	-0.87272	-1.21538	0.29140
C	-2.20593	-1.20957	-0.11555
C	-2.87186	-0.00006	-0.31972
H	-2.72498	2.15452	-0.27191

H	-0.33993	2.15221	0.45385
H	-0.33971	-2.15224	0.45343
H	-2.72477	-2.15463	-0.27235
H	-3.91415	-0.00008	-0.63750
N	1.16965	-0.00000	0.88064
C	2.24942	0.00006	-0.30381
O	3.38730	-0.00028	0.15817
O	1.75361	0.00044	-1.42185
H	1.38935	-0.81973	1.45411
H	1.38929	0.81969	1.45420

Se_dianion

Se	0.000000	0.000000	0.000000

Ground states structures of salenocarbate tautomers

3a

C	1.121662	0.504674	-0.036884
O	0.916706	1.720390	-0.141648
Se	2.878223	-0.263707	0.015612
N	0.099095	-0.403496	0.049422
H	0.391396	-1.370774	0.092916
C	-1.293314	-0.195505	0.024650
C	-2.095598	-1.346779	-0.039345
C	-1.906687	1.063396	0.076774
C	-3.481902	-1.242471	-0.054457
H	-1.620539	-2.328222	-0.077039
C	-3.300272	1.152173	0.058742
H	-1.305993	1.964622	0.132746
C	-4.097023	0.010944	-0.007334
H	-4.085332	-2.149074	-0.104791
H	-3.764152	2.138163	0.100213
H	-5.183482	0.094073	-0.020505

3b

C	1.453743	1.030876	0.025394
O	2.572282	1.603817	0.048342
Se	1.702713	-0.969958	-0.030035
N	0.282645	1.583342	0.028698
C	-0.907656	0.843773	0.018092
C	-1.509673	0.435658	1.218994
C	-1.553958	0.543589	-1.191285
C	-2.711206	-0.271682	1.207729
H	-1.019116	0.672087	2.163849
C	-2.755827	-0.163668	-1.198872

H	-1.098291	0.863655	-2.128937
C	-3.340727	-0.578184	-0.000538
H	-3.158829	-0.586394	2.151392
H	-3.238371	-0.393939	-2.149704
H	-4.280000	-1.131242	-0.007913
H	0.297424	-1.401691	-0.072194

3c

C	-1.378644	0.873480	0.000084
O	-2.481455	1.686694	0.000196
Se	-1.730540	-0.998740	-0.000105
N	-0.259915	1.495332	0.000144
C	0.949427	0.777371	0.000075
C	1.579166	0.448415	-1.207675
C	1.578979	0.447827	1.207764
C	2.807198	-0.212447	-1.204952
H	1.096232	0.711577	-2.149203
C	2.807011	-0.213033	1.204909
H	1.095898	0.710529	2.149344
C	3.428224	-0.547312	-0.000055
H	3.282938	-0.465799	-2.153178
H	3.282603	-0.466848	2.153085
H	4.389146	-1.061841	-0.000106
H	-3.265579	1.122872	0.000135

3a·H (NH₂)

C	1.10342	0.00029	-0.43925
O	0.56736	0.00072	-1.51842
Se	2.87376	-0.00012	0.07714
N	0.11096	0.00005	0.78888
H	0.35419	-0.81929	1.35578
C	-1.30581	-0.00003	0.45385
C	-1.95484	-1.21678	0.28370
C	-1.95505	1.21666	0.28412
C	-3.30503	-1.21033	-0.06226
H	-1.41372	-2.15269	0.42156
C	-3.30525	1.21010	-0.06185
H	-1.41411	2.15263	0.42231
C	-3.97864	-0.00015	-0.23476
H	-3.83089	-2.15495	-0.19571
H	-3.83127	2.15467	-0.19496
H	-5.03453	-0.00020	-0.50387
H	0.35403	0.81932	1.35593

3a·H (SeH)

C	-1.05993	0.51406	0.01937

O	-0.91227	1.72470	0.09903
Se	-2.83275	-0.30099	-0.00695
N	-0.06718	-0.40324	-0.05594
H	-0.35124	-1.37532	-0.09884
C	1.33135	-0.19490	-0.02878
C	2.12908	-1.34654	0.02485
C	1.93422	1.06714	-0.06327
C	3.51510	-1.23798	0.04757
H	1.65517	-2.32873	0.04881
C	3.32727	1.15936	-0.03783
H	1.33171	1.96790	-0.11091
C	4.12468	0.01815	0.01813
H	4.12132	-2.14280	0.08968
H	3.78938	2.14632	-0.06453
H	5.21075	0.10395	0.03745
H	-3.48586	1.01177	0.05371

Transition states structures
TS1
Imaginary frequency: -253.99 cm⁻¹

C	-2.133579	0.642670	0.007095
O	-2.757294	1.624120	0.021119
Se	-1.680152	-1.032795	-0.142013
N	0.040034	1.833819	0.560721
H	-0.156984	2.392147	-0.271872
C	1.091040	1.026221	0.287247
C	1.753232	0.956281	-0.979003
C	1.583675	0.127877	1.283566
C	2.812398	0.085474	-1.211751
H	1.409856	1.614016	-1.782140
C	2.642364	-0.739575	1.036986
H	1.107765	0.135540	2.266989
C	3.278970	-0.777260	-0.210724
H	3.284907	0.075977	-2.196969
H	2.980635	-1.403456	1.836186
H	4.108493	-1.459003	-0.398247

TS1'
Imaginary frequency: -275.70 cm⁻¹

C	1.402901	1.461480	0.169552
O	2.538591	1.818659	0.266044
Se	1.592616	-1.118150	-0.188516
N	0.192328	1.754018	0.126313
C	-0.931034	0.916457	0.097382
C	-1.280787	0.149623	1.215204
C	-1.740707	0.891610	-1.043076

C	-2.420167	-0.653068	1.178765
H	-0.655143	0.186045	2.106342
C	-2.878960	0.087320	-1.071222
H	-1.468604	1.498818	-1.905990
C	-3.222381	-0.689178	0.037069
H	-2.682844	-1.251869	2.051124
H	-3.500678	0.067900	-1.966602
H	-4.113264	-1.316588	0.012378
H	3.043379	-0.980054	-0.402286

TS2
Imaginary frequency: -243.42 cm^{-1}

C	1.402901	1.461480	0.169552
O	2.538591	1.818659	0.266044
Se	1.592616	-1.118150	-0.188516
N	0.192328	1.754018	0.126313
C	-0.931034	0.916457	0.097382
C	-1.280787	0.149623	1.215204
C	-1.740707	0.891610	-1.043076
C	-2.420167	-0.653068	1.178765
H	-0.655143	0.186045	2.106342
C	-2.878960	0.087320	-1.071222
H	-1.468604	1.498818	-1.905990
C	-3.222381	-0.689178	0.037069
H	-2.682844	-1.251869	2.051124
H	-3.500678	0.067900	-1.966602
H	-4.113264	-1.316588	0.012378
H	3.043379	-0.980054	-0.402286

TS 3c
Imaginary frequency: -315.87 cm^{-1}

C	1.14418	-0.20972	-0.03588
O	0.71355	1.67186	1.23685
Se	2.91422	-0.15983	-0.13669
N	0.05279	-0.67599	-0.22552
C	-1.30844	-0.37933	-0.16357
C	-1.78689	0.82234	-0.69759
C	-2.18289	-1.30951	0.40286
C	-3.15151	1.09572	-0.64073
H	-1.09093	1.52625	-1.15073
C	-3.54470	-1.01944	0.45866
H	-1.79194	-2.24490	0.80079
C	-4.03252	0.18049	-0.06133
H	-3.52775	2.03098	-1.05475
H	-4.22805	-1.73923	0.90873
H	-5.09893	0.40079	-0.01904

H	-0.24714	1.73413	1.27194

TS 3a·H (NH₂)
Imaginary frequency: -304.30 cm^{-1}

C	-1.28409	0.00028	0.62609
O	-0.55669	0.00067	1.54128
Se	-2.92323	-0.00007	-0.05975
N	0.02044	-0.00027	-1.02462
H	-0.24951	-0.83405	-1.53936
C	1.36814	-0.00018	-0.60745
C	2.01884	-1.21153	-0.35563
C	2.01886	1.21129	-0.35626
C	3.32486	-1.20640	0.13037
H	1.50063	-2.15225	-0.54494
C	3.32488	1.20641	0.12974
H	1.50065	2.15192	-0.54605
C	3.98379	0.00006	0.37494
H	3.83056	-2.15346	0.31961
H	3.83059	2.15355	0.31849
H	5.00505	0.00016	0.75507
H	-0.24947	0.83320	-1.53987

TS3
Imaginary frequency: -223.06 cm^{-1}

C	2.433530	0.875254	0.520216
C	1.112665	1.296550	0.369040
C	0.182333	0.459125	-0.251698
C	0.583212	-0.789562	-0.742081
C	1.905022	-1.201338	-0.587155
C	2.835292	-0.373502	0.045018
H	3.152407	1.531265	1.011465
H	0.795237	2.272200	0.735773
H	-0.143894	-1.429408	-1.240628
H	2.210199	-2.176165	-0.968058
H	3.868709	-0.699175	0.162270
N	-1.129387	0.923769	-0.428970
C	-2.225844	0.395545	-0.273850
O	-3.393640	0.242785	-0.357155
O	-1.860057	-1.310344	1.289894
H	-0.904632	-1.397062	1.363121

TS3'
Imaginary frequency: -277.83 cm^{-1}

C	-2.553782	-1.158879	0.047830
C	-1.170720	-1.331417	0.058868
C	-0.326514	-0.218123	0.004913

C	-0.875818	1.068381	-0.063761
C	-2.260219	1.230728	-0.076508
C	-3.105605	0.121353	-0.020275
H	-3.203466	-2.033276	0.091662
H	-0.735461	-2.329016	0.110259
H	-0.227225	1.943480	-0.109973
H	-2.679473	2.235561	-0.132014
H	-4.187208	0.254325	-0.030665
N	1.069698	-0.463714	0.011931
C	1.915633	0.432913	0.057980
O	2.515007	1.443255	0.128013
O	3.794479	-0.933447	-0.114204
H	3.331215	-1.773275	-0.177532

TS4
Imaginary frequency: **-114.79 cm**$^{-1}$

C	2.104621	1.252844	-0.220894
C	0.867073	0.906861	-0.750452
C	0.314295	-0.406324	-0.601564
C	1.130629	-1.326319	0.136007
C	2.367702	-0.965190	0.657848
C	2.881856	0.328449	0.492066
H	2.476758	2.269871	-0.368222
H	0.288231	1.650562	-1.303399
H	0.760093	-2.344483	0.284921
H	2.947154	-1.710173	1.209123
H	3.852423	0.606259	0.903044
N	-0.896104	-0.701326	-1.124371
C	-2.711754	0.305473	0.396322
O	-2.140220	1.288004	0.664785
O	-3.443391	-0.595757	0.259387
H	-1.109575	-1.675501	-0.904237

TS4'
Imaginary frequency: **-191.67 cm**$^{-1}$

C	2.248310	-1.088771	0.774268
C	0.950916	-0.977344	0.285006
C	0.553786	0.111138	-0.545639
C	1.567175	1.070378	-0.840356
C	2.861463	0.944931	-0.345900
C	3.226316	-0.133604	0.469673
H	2.504710	-1.941410	1.407177
H	0.209425	-1.738037	0.537041
H	1.310646	1.922785	-1.474666
H	3.602964	1.705351	-0.601578
H	4.241505	-0.227047	0.855314

N	-0.727459	0.193690	-0.993611
C	-2.302667	0.767492	0.764416
O	-1.763131	0.248912	1.665600
O	-3.044671	1.357829	0.074970
H	-1.672048	-1.139241	-1.039620
O	-2.260507	-1.972634	-1.041188
H	-2.354439	-2.193107	-0.108955
H	-0.835867	1.016706	-1.583316

TS5
Imaginary frequency: **-316.81 cm**$^{-1}$

C	-2.226862	-1.199514	0.196353
C	-0.928169	-1.222062	-0.309375
C	-0.277019	-0.020903	-0.598479
C	-0.919042	1.198588	-0.372366
C	-2.217720	1.212058	0.133700
C	-2.877137	0.015375	0.420478
H	-2.733207	-2.139480	0.416681
H	-0.416667	-2.169618	-0.482648
H	-0.400499	2.132041	-0.594081
H	-2.716914	2.165953	0.304987
H	-3.892281	0.029503	0.816458
N	1.069477	-0.037200	-1.043490
C	2.439652	0.015362	0.453620
O	3.470128	-0.015666	-0.139012
O	1.792703	0.060601	1.447588
H	1.304943	0.772944	-1.612233
H	1.303421	-0.883849	-1.556922

Mass Spectra
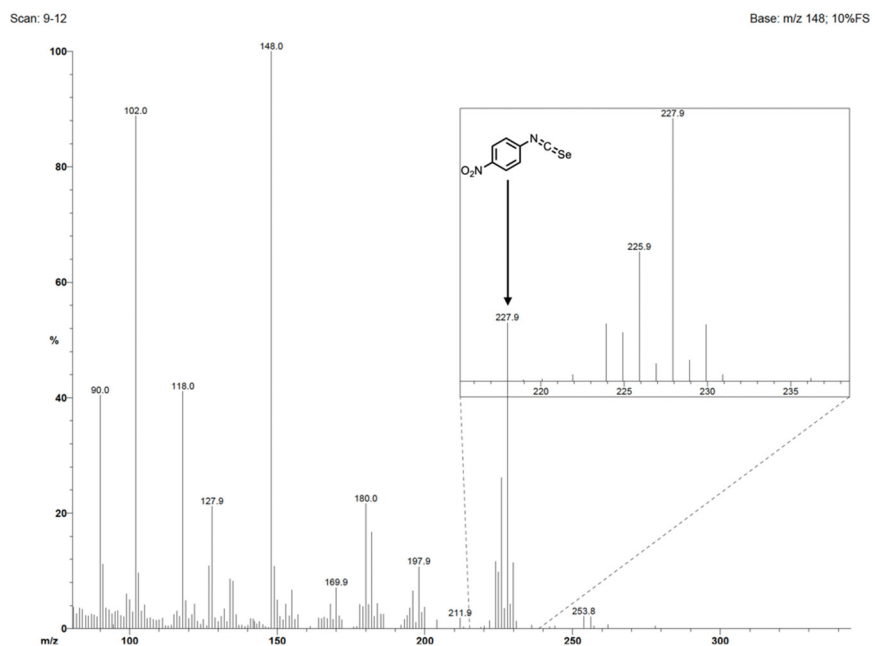
Figure S26. Mass spectrum (EI-MS) of 4-nitroformanilide. Actual mass: m/z 227.9438 ([$C_7H_4N_2O_2Se$]$^-$), calculated 227.9434.
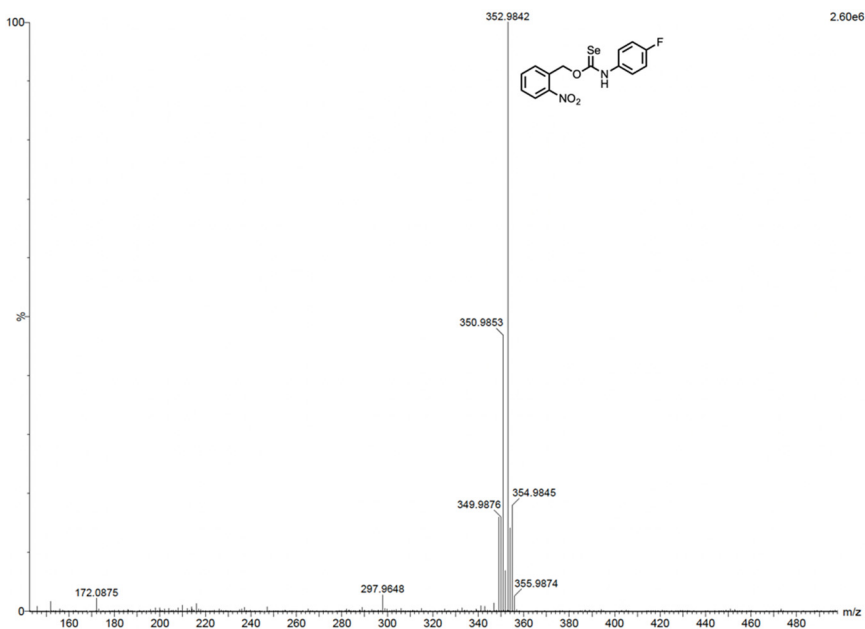

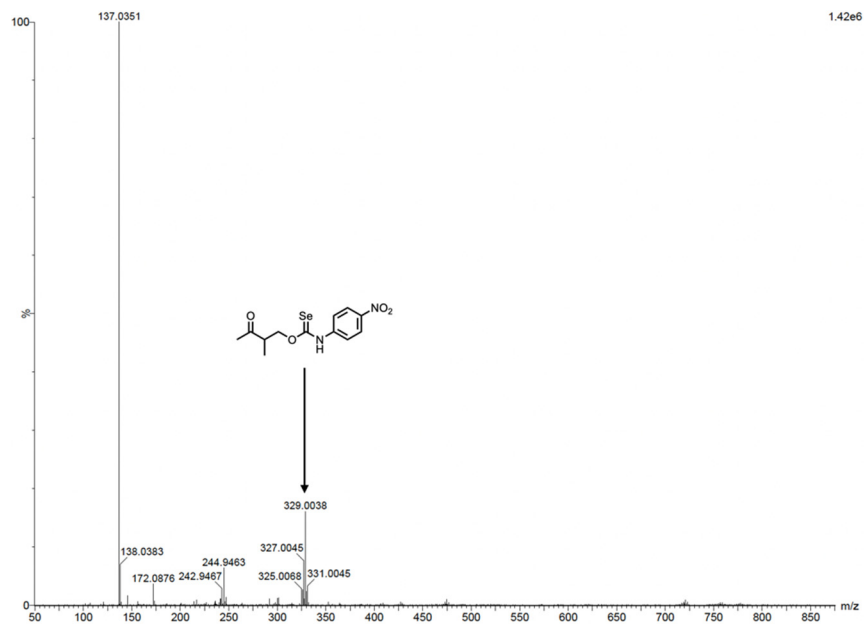**Figure S27.** Mass spectrum (ESI-MS) of PhotoSeCM. Actual mass: m/z 352.9842 ([$C_{14}H_{10}FN_2O_3Se$]$^-$), calculated 352.9841.

Figure S28. Mass spectrum (ESI-MS) of PNA-MeGKSeCM. Actual mass: m/z 329.0038 ($[C_{12}H_{13}N_2O_4Se]^-$), calculated 329.0041.
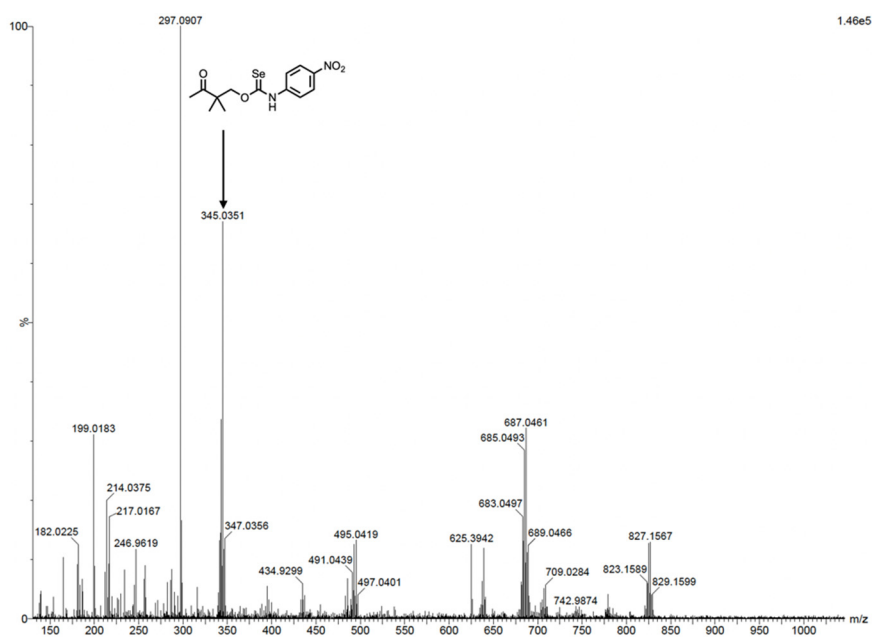

Figure S29. Mass spectrum (ESI-MS) of PNA-Me$_2$GKSeCM. Actual mass: m/z 345.0351 ($[C_{13}H_{16}N_2O_4Se]^+$), calculated 345.0354.
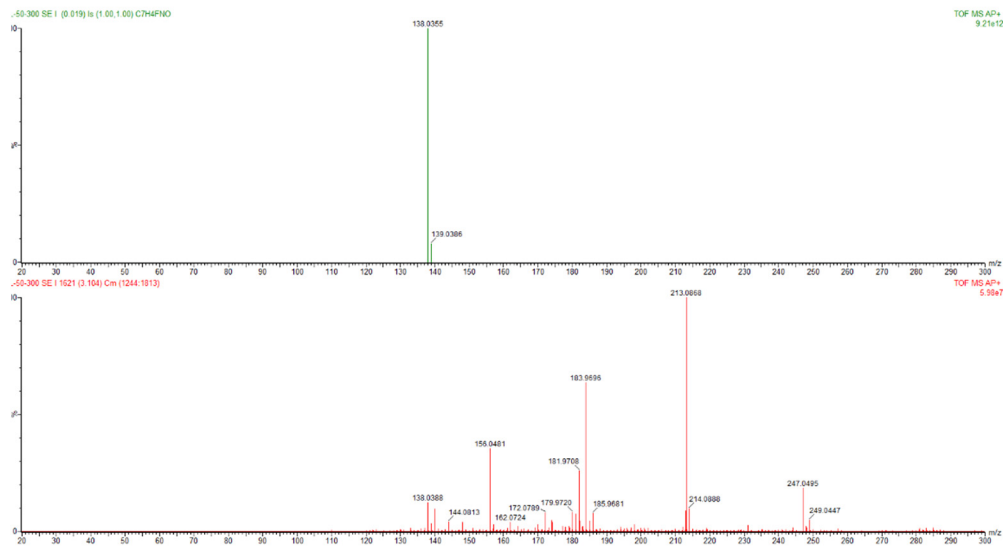
Figure S30. Mass spectrum (API-MS) of the crude product mixture after irradiation products of PhotoSeCM showing *p*-fluoroisocyanate formation. Actual mass of *p*-fluoroisocyanate (bottom) : m/z 138.0388 ([C_7H_5FNO]$^+$), calculated mass (top) 138.0355.

References

1. Gaussian 16, Revision C.01, M. J. Frisch, G. W. Trucks, H. B. Schlegel, G. E. Scuseria, M. A. Robb, J. R. Cheeseman, G. Scalmani, V. Barone, G. A. Petersson, H. Nakatsuji, X. Li, M. Caricato, A. V. Marenich, J. Bloino, B. G. Janesko, R. Gomperts, B. Mennucci, H. P. Hratchian, J. V. Ortiz, A. F. Izmaylov, J. L. Sonnenberg, D. Williams-Young, F. Ding, F. Lipparini, F. Egidi, J. Goings, B. Peng, A. Petrone, T. Henderson, D. Ranasinghe, V. G. Zakrzewski, J. Gao, N. Rega, G. Zheng, W. Liang, M. Hada, M. Ehara, K. Toyota, R. Fukuda, J. Hasegawa, M. Ishida, T. Nakajima, Y. Honda, O. Kitao, H. Nakai, T. Vreven, K. Throssell, J. A. Montgomery, Jr., J. E. Peralta, F. Ogliaro, M. J. Bearpark, J. J. Heyd, E. N. Brothers, K. N. Kudin, V. N. Staroverov, T. A. Keith, R. Kobayashi, J. Normand, K. Raghavachari, A. P. Rendell, J. C. Burant, S. S. Iyengar, J. Tomasi, M. Cossi, J. M. Millam, M. Klene, C. Adamo, R. Cammi, J. W. Ochterski, R. L. Martin, K. Morokuma, O. Farkas, J. B. Foresman, and D. J. Fox, Gaussian, Inc., Wallingford CT, 2019.

2. Chai, J.-D.; Head-Gordon, M., Long-range corrected hybrid density functionals with damped atom–atom dispersion corrections. *Phys. Chem. Chem. Phys.* **2008,** *10* (44), 6615-6620.

3. Dunning Jr, T. H.; Peterson, K. A.; Wilson, A. K., Gaussian basis sets for use in correlated molecular calculations. X. The atoms aluminum through argon revisited. *The Journal of Chemical Physics* **2001,** *114* (21), 9244-9253.

4. Marenich, A. V.; Cramer, C. J.; Truhlar, D. G., Universal solvation model based on solute electron density and on a continuum model of the solvent defined by the bulk dielectric constant and atomic surface tensions. *The Journal of Physical Chemistry B* **2009,** *113* (18), 6378-6396.

5. Bootsma, A. N.; Wheeler, S., Popular integration grids can result in large errors in DFT-computed free energies. **2019**.

6. Funes-Ardoiz, I.; Paton, R. S., GoodVibes version 2.0. 3. *O O NH4++ formation of heterocycles containing CN bonds O O NH3+-H* **2018**.

7. Grimme, S., Supramolecular binding thermodynamics by dispersion-corrected density functional theory. *Chemistry–A European Journal* **2012,** *18* (32), 9955-9964.

8. Legault, C., CYLview, 1.0 b. Université de Sherbrooke 2009

9. Watt, S. K. I.; Charlebois, J. G.; Rowley, C. N.; Keillor, J. W., A mechanistic study of thiol addition to N-acryloylpiperidine. *Org. Biomol. Chem.* **2023,** *21* (10), 2204-2212.

10. Humeres, E.; Sun Lee, B.; Debacher, N. A., Mechanisms of Acid Decomposition of Dithiocarbamates. 5. Piperidyl Dithiocarbamate and Analogues. *J. Org. Chem.* **2008,** *73* (18), 7189-7196.